Geobiology

Geobiology (2014), **12**, 250–264 DOI: 10.1111/gbi.12082

Prokaryote populations of extant microbialites along a depth gradient in Pavilion Lake, British Columbia, Canada

J. A. RUSSELL,[1] A. L. BRADY,[2,*] Z. CARDMAN,[3] G. F. SLATER,[4] D. S. S. LIM[5,6] AND J. F. BIDDLE[1]

[1]*School of Marine Science and Policy, University of Delaware, Lewes, DE, USA*
[2]*Department of Biological Sciences, University of Calgary, Calgary, AB, Canada*
[3]*University of North Carolina at Chapel Hill, Chapel Hill, NC, USA*
[4]*School of Geography and Earth Sciences, McMaster University, Hamilton, ON, Canada*
[5]*NASA Ames Research Center, Moffet Field, CA, USA*
[6]*SETI Institute, Mountain View, CA, USA*

ABSTRACT

Pavilion Lake in British Columbia, Canada, is home to modern-day microbialites that are actively growing at multiple depths within the lake. While microbialite morphology changes with depth and previous isotopic investigations suggested a biological role in the formation of these carbonate structures, little is known about their microbial communities. Microbialite samples acquired through the Pavilion Lake Research Project (PLRP) were first investigated for phototrophic populations using *Cyanobacteria*-specific primers and 16S rRNA gene cloning. These data were expounded on by high-throughput tagged sequencing analyses of the general bacteria population. These molecular analyses show that the microbial communities of Pavilion Lake microbialites are diverse compared to non-lithifying microbial mats also found in the lake. Phototrophs and heterotrophs were detected, including species from the recently described *Chloroacidobacteria* genus, a photoheterotroph that has not been previously observed in microbialite systems. Phototrophs were shown as the most influential contributors to community differences above and below 25 meters, and corresponding shifts in heterotrophic populations were observed at this interface as well. The isotopic composition of carbonate also mirrored this shift in community states. Comparisons to previous studies indicated this population shift may be a consequence of changes in lake chemistry at this depth. Microbial community composition did not correlate with changing microbialite morphology with depth, suggesting something other than community changes may be a key to observed variations in microbialite structure.

Received 3 December 2013; accepted 29 January 2014

Corresponding author: J. F. Biddle. Tel.: 302 645 4267; fax: 302 645 4007; e-mail: jfbiddle@udel.edu

*Present address: School of Geography and Earth Sciences, McMaster University, Hamilton, ON, Canada

INTRODUCTION

Microbialites are generally defined as organosedimentary structures formed through lithification of a sediment/biomass matrix by micro-organsims in a microbial mat (Burne & Moore, 1987; Reid *et al.*, 2000; Dupraz & Visscher, 2005). This lithification can be caused by either phototrophic or heterotrophic activity, or by a combination of the two (Dupraz & Visscher, 2005; Dupraz *et al.*, 2009). Among the earliest evidence of life on Earth are fossilized microbialite structures, dated at 3.4 Ga, which are the dominant sign of biological activity in the fossil record for nearly 85% of Earth's history (Lowe, 1980; Schopf & Packer, 1987; Grotzinger & Knoll, 1999). Extant analogs of these structures still exist throughout the world (Arp *et al.*, 1999; Abed *et al.*, 2003; Gischler *et al.*, 2008; Breitbart *et al.*, 2009; Foster *et al.*, 2009). The study of microbialites offers a unique opportunity to more fully understand Earth's earliest life.

Pavilion Lake is host to one of the largest concentrations of freshwater microbialites in the world (Fig. 1, Laval *et al.*, 2000). It is a temperate lake surrounded by karst

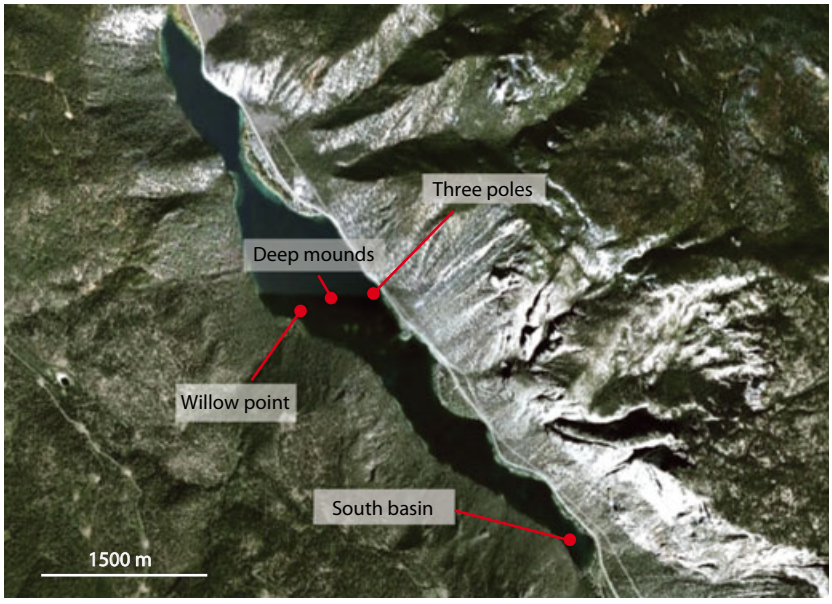

Fig. 1 Map of Pavilion Lake showing four sample collection sites. Scale bar in lower left. Deep mounds are located at 50°51′52.77″N, 121°44′15.23″W.

hydrogeology, slightly alkaline and considerably oligotrophic, yet still harbors metazoan grazers, typically considered an inhibitor of microbialite growth (Lim *et al.*, 2009). Even more interesting is the vast array of microbialite morphologies varying with depth throughout the lake. Shallower microbialites (10–15 m depth) are small (centimeter to meter scale), light in color, friable, and often form bunched cauliflower shapes. Intermediate depth (15–25 m depth) structures exhibit larger, meter-scale mounds occasionally topped by conical-shaped hollow chimneys. Deep microbialites (25–45 m depth) are a dark green-brown color, more dense, and form various artichoke shapes (Fig. S1, Laval *et al.*, 2000). More recently discovered deep mound microbialites (45–55 m) exhibit morphologies and dark colorations that are distinct from those microbialites previously identified (Lim *et al.*, 2009, 2011). Non-lithifying microbial mats have also been observed at shallow depths (3 m) in Pavilion Lake (Lim *et al.*, 2009).

Initial microscopic investigations of the microbes on the surface of Pavilion Lake microbialites indicated *Cyanobacteria* to be the most dominant phylum of the community. Specifically, *Gloeocapsa* sp., *Synechococcus* sp., and *Pseudoanabaena* sp. comprised the majority of the visible mat species, interspersed with purple-colored globular clusters of *Calothrix* sp. and *Oscillatoria* sp. (Laval *et al.*, 2000). *Cyanobacteria* have been shown to be the dominant members of many microbialite communities (Reid *et al.*, 2000; Burns *et al.*, 2004; Havemann & Foster, 2008; Allen *et al.*, 2009; Breitbart *et al.*, 2009; Foster & Green, 2011). Heterotrophs are also expected to play an important role in the lithification of layers in these structures (Dupraz & Visscher, 2005; Dupraz *et al.*, 2009). It has been proposed that microbialite accretion depends on a complex balance between photoautotrophy and heterotrophic respiration (Pinckney & Reid, 1997).

The common model of microbialite growth starts with a pioneer cyanobacterial mat community and the buildup of exopolymeric substance (EPS), a mucosal slime that has many functions including adhesion to a surface, protection against dessication, scavenging of trace metals, and anticalcification (Decho, 1990). The EPS matrix binds Ca^{2+} ions in the water, most often seeded by heavy sedimentation, inhibiting $CaCO_3$ precipitation. Eventually, the upper limit of EPS concentration in the system is reached, and it experiences one of three fates: degradation by heterotrophic respiration, organomineralization reorganizing acid binding sites, or saturation of Ca^{2+} binding sites. All three of these scenarios lead to the precipitation of $CaCO_3$, and the first two can be directly mediated by micro-organisms (Dupraz & Visscher, 2005). Thus, while it is possible to have microbialite accretion through phototrophic microbes alone, it is likely that heterotrophic populations are also involved.

Microbial metabolic activity has the potential to influence local geochemical environments creating conditions favorable for carbonate precipitation with both autotrophic and heterotrophic processes contributing to microbialite formation (Merz, 1992 Visscher *et al.*, 2000; Ludwig *et al.*, 2005; Bonilla- Rosso *et al.*, 2012; Peimbert *et al.*, 2012). These geochemical changes impact the ^{13}C isotopic composition of the local dissolved inorganic carbon (DIC), and carbonate precipitated from this source preserves these changes as a biosignature of microbial activity (Sumner, 2001). Photoautotrophic activity is thought to promote carbonate precipitation via the use of carbonic anhydrase to uptake and convert HCO_3^- to CO_2 resulting in the

release of OH^- into the medium leading to an associated rise in pH and consequently carbonate supersaturation and precipitation (Revsbech *et al.*, 1983; Merz, 1992; Shiraiwa *et al.*, 1993). The concurrent photosynthetic drawdown of ^{12}C from the DIC pool leaves the residual DIC pool enriched in ^{13}C (O'Leary 1988, Hollander & Mckenzie, 1991). Carbonate precipitated from this DIC pool records the influence of phototrophy on the system as measured $\delta^{13}C$ values that are higher than predicted for abiotic precipitation in equilibrium with ambient DIC. Heterotrophic activity also raises the saturation index but in contrast to photosynthesis, inputs ^{13}C-depleted HCO_3^- to the DIC pool as a result of respiration activities that involve minimal fractionation from the organic matter source (Altermann *et al.*, 2006; Andres *et al.*, 2006; Baumgartner *et al.*, 2006). The measured $\delta^{13}C$ value of carbonate reflects the balance of autotrophic and heterotrophic inputs. The direction of deviation of the $\delta^{13}C$ of carbonate minerals from the predicted equilibrium abiotic values provides insight into dominant metabolic processes. Biosignatures of heterotrophic influences on carbonate precipitation have been detected in some marine (e.g., Andres *et al.*, 2006) and freshwater microbialite systems (e.g., Breitbart *et al.*, 2009; Bonilla- Rosso *et al.*, 2012; Peimbert *et al.*, 2012). Phototrophic influence on carbonate precipitation, as reflected in ^{13}C-enriched $\delta^{13}C$ values, has also been identified in lacustrine systems (Hollander & Mckenzie, 1991; Thompson *et al.*, 1997).

Recent work has shown that Pavilion Lake microbialites have a photoautotrophic origin. Analysis of $\delta^{13}C$ values from both DIC and associated carbonate in nodular clumps of microbial biomass on the surface of the microbialites was consistent with biotic precipitation of carbonate via photosynthesis (Brady *et al.*, 2010). It is possible that heterotrophic respiration makes important contributions to microbialite accretion in Pavilion Lake, as seen in other marine and freshwater microbialite systems (Foster & Green, 2011), but it has not yet been identified in Pavilion Lake. How the phototroph/heterotroph consortia are distributed with depth and what, if any, affect they have on the diverse microbialite morphologies seen in Pavilion Lake is currently unknown. Analyses of these communities with advanced molecular biological tools paired with isotope geochemistry will allow a more robust understanding of their diversity, function, and distribution.

In this study, multiple molecular analyses were used to investigate the microbial communities within a comprehensive sample set of Pavilion Lake's lithified microbialites, non-lithifying soft mats, and nodular growths. We hypothesize that microbial community change would be gradual along a depth gradient, influenced heavily by changing photosynthetically active radiation (PAR) availability and correlated to changes in microbialite morphology. However, a community structure that separates microbialites above and below 25 m is seen and is supported by isotopic data. Additionally, significant community differences are observed between non-lithifying soft mats and lithifying microbialites, despite some abundant operational taxonomic units (OTUs) being shared across all samples. The association of microbial taxa with specific depths and mat morphology and the balance of known phototrophs vs. known heterotrophs across depths are discussed.

METHODS

Sample collection

Samples were collected via SCUBA diver and Deep worker submersible, from depths ranging between 3–45 m, during summers between 2007–2010 (Lim *et al.*, 2011). Diver-collected samples were placed in plastic bags along with surrounding bottom water and brought to the surface. Deep worker samples were collected by robotic arm and placed in a basket and brought to the surface. On shore, samples were photographed and measured, then sectioned with sterile tools. Sectioned samples were placed in sterile Whirl-pak bags and frozen at −20 °C. Nodules were collected from individual microbialites and pooled by colors previously identified in Brady *et al.*, 2010. Samples were shipped on dry ice and stored at −80 °C until further laboratory analysis. A total of 19 samples were investigated, including microbialites, soft mats, and nodules (Table 1, Fig. S1).

Table 1 Sample locations, depths, and details

Sample name	Collection site	Depth (meters)	Collection date	Type of sample
PLRP.3	Three poles	26	July 9, 2009	Microbialite
PLRP.4	Three poles	11	July 9, 2009	Microbialite
PLRP.6	Three poles	21	July 13, 2009	Microbialite
PLRP.7	Three poles	12	July 13, 2009	Microbialite
PLRP.8	Three poles	12	July 13, 2009	Microbialite
PLRP.9	Deep mound	45	July 14, 2009	Microbialite
PLRP.10	Deep mound	45	July 14, 2009	Microbialite
PLRP.11	Three poles	26	July 3, 2010	Microbialite
PLRP.12	Three poles	18	July 3, 2010	Microbialite
PLRP.15	South Basin	3	July 14, 2009	Soft mat
PLRP.16	South basin	3	July 14, 2009	Soft mat
PLRP.17	South basin	3	July 14, 2009	Soft mat
PLRP.19	Three poles	11	July 9, 2009	Microbialite
PLRP.20	Willow point	32	July 14, 2009	Microbialite
Nod.1	Three poles	20	July 4, 2010	Nodule
Nod.2	Three poles	20	July 4, 2010	Nodule
Nod.5	Three poles	20	April 23, 2008	Nodule
Nod.6	Three poles	11	October 17, 2008	Nodule
Nod.7	Willow point	20	June 22, 2007	Nodule

PLRP, Pavilion Lake Research Project.

DNA extraction, amplification, and sequencing

Extraction

Genetic material was isolated from microbialite samples, nodule samples, and soft mat samples as follows: From microbialites, 2 g of sample from the outer surface was broken off and crushed in a sterilized rock crusher to a coarse (~1 mm) grain size; from either this crushed 2 g sample or 2 g of soft mat or ~0.25 g of pooled nodules, DNA was isolated using the MoBio PowerSoil DNA Isolation kit (MoBio Labs, Carlsbad, CA, USA) according to the manufacturer's instructions, except for the cell lysing step which used a FastPrep-24 Cell Homogenizer for 40 s (MP Biomedicals, Santa Ana, CA, USA). An extraction control was processed with all samples.

Amplification and Sanger sequencing

Microbialite and soft mat samples were amplified using the *Cyanobacteria*-specific primers Cya359F/Cya781R (Nübel *et al.*, 1997). Nodule 16S rRNA genes were amplified using general bacterial primers targeting B27F/B338R (Lane, 1991). Reagents included 2 μL 10× FB1 Buffer (Takara Bio, Mountain View, CA, USA), 2 μL dNTPs, 0.8 μM of each primer, 0.5 μL Takara SpeedStar polymerase (Takara Bio), template (~20 ng), and dH_2O for a total reaction volume of 25 μL. PCRs were run on an Eppendorf Mastercycler Pro thermocycler (Eppendorf Inc., Hamburg, Germany). The PCR cycling conditions were: 94 °C for 2 min; 25 cycles of 94 °C for 15 s, 57 °C for 15 s, 72 °C for 30 s; 72 °C for 2 min. PCR products were checked for correct size by gel electrophoresis in a 1% agarose gel. In all experiments, the negative control showed no product. PCR products were ligated into pCR 2.1 TOPO cloning vector and transformed into chemically competent *E. coli* cells via the TOPO TA Cloning Kit for Sequencing (Invitrogen, Inc., Carlsbad, CA, USA). After overnight incubation at 37 °C on LB/Xgal/Kanamycin agar plates, insert-positive colonies were picked and replated for sequencing (GENEWIZ Inc., South Plainfield, NJ, USA) using plasmid primers.

454 Pyrosequencing

Extracted DNA from microbialites and soft mats was also used in a pyrosequencing analysis of community 16S rRNA genes. The same general bacterial primers were used as above; however, each reverse primer was modified with a unique 8 bp barcode as well as a library A adapter for Roche 454 Titanium chemistry (Meyer *et al.*, 2007). PCR product was checked via electrophoresis in 1% agarose gel. The negative control showed no sign of product. Correct size gel bands were extracted and purified with the Wizard SV Gel and PCR Clean-Up System (Promega, Inc., Madison, WI, USA). DNA concentration was checked on a NanoDrop 2000c Spectrophotometer (Thermo Scientific Inc., Waltham, MA, USA). Equimolar amounts of tagged PCR product from each sample were pooled and sent for sequencing via Roche 454 pyrosequencing using *Titanium* chemistry (EngenCore, Columbia, SC, USA).

Sequence analysis

Sanger sequences were trimmed in Sequencher (Gene Codes Inc., Ann Arbor, MI, USA). Chimeric sequences were identified and discarded using the chimera.check command in Mothur (Schloss *et al.*, 2009). Sequences were initially characterized using BLAST (Altschul *et al.*, 1990), using the NR/NT database. Further taxonomic analysis was performed with the open-source QIIME software package (Caporaso *et al.*, 2010) as well as the ARB platform for trees (Ludwig *et al.*, 2004). The 454-generated sequences were denoised prior to further analysis using the QIIME pyrosequencing denoiser algorithm. After quality filtering the data, sequences were rarified to the level of the least robust sample to avoid sample bias. Sequences were randomly subsampled from each sample from sequencing efforts as follows: $N = 5900$ for pyrosequenced microbialite, $N = 600$ for pyrosequenced soft mat samples, $N = 20$ for Sanger-sequenced samples of nodules, $N = 12$ for Sanger-sequenced microbialite and soft mat samples. Sequences were only compared within similar primers and sequencing type. Random subsampling of sequences was completed in QIIME using the *multiple_rarefactions.py* script, with 10 iterations of each of the four sequencing efforts. OTU tables were generated for each iteration at 97% identity level. Taxonomic profiles were assigned using the SILVA database and did not change across iterations. Sequences have been deposited into the NCBI database under accession numbers SRX450588 - SRX450600, and TI2337798042-2337790186.

Statistical analyses

Chao richness indices were calculated in the QIIME pipeline. PRIMER-E 6th Edition (Primer-E Ltd., Plymouth, UK) was used to calculate Bray–Curtis resemblance matrices, cluster analyses, and multidimensional scaling (MDS) plots. The RELATE statistical test in Primer-E was also applied to resemblance matrices of the various OTU tables generated in this study (Sanger clones targeting *Cyanobacteria*, pyrosequencing of the total community, subsets of the pyrosequencing data, etc.) and compared to a modeled matrix based on depth categories ≤21 m and ≥26 m. Outputs of this analysis included a correlation coefficient (ρ) and a significance value (P); a rho value of 1 would indicate a high fidelity model. Individual OTU influence toward the depth categories described above was determined via SIMPER analysis in Primer-E *6th Edition* (Primer-E Ltd., Plymouth, UK). The SIMPER program, short for

'similarity percentages', converts Bray–Curtis dissimilarities between all pairs of samples into percentage contribution of each species to the dissimilarity seen between groups or to the similarity within groups. For SIMPER analysis in this study, the 'groups' were the depth categories discussed above (≤21 m and ≥26 m). Like the RELATE test, SIMPER acts on the high-dimensional structure of the Bray–Curtis matrix and thus gives a more accurate interpretation of community structure than can be seen via MDS (Clarke & Gorley, 2006).

Isotope analyses

Subsamples for carbonate analysis were collected from the surface of three individual microbialites recovered from each distinct depth ranging from 11 to 45 meters. Carbonate stable isotope analyses were performed on an Optima isotope ratio mass spectrometer with an Isocarb common acid bath at 90 °C at McMaster University. Triplicate analysis of carbonate samples gave precisions of less ± 0.2‰ (1 σ) for $\delta^{13}C_{carb}$. Carbonate $\delta^{13}C_{carb}$ values are reported relative to PeeDee Belemnite (PDB). The range of carbonate $\delta^{13}C$ values expected for abiotic equilibrium precipitation was determined based on the average of measured Pavilion Lake DIC $\delta^{13}C$ values (Brady *et al.*, 2009, 2010).

RESULTS

A total of 19 samples were investigated from Pavilion Lake, including microbialites, soft mats, and nodules originating from four sampling locations (Fig. 1). The samples were distributed along the depth gradient in the lake (Fig. S1). To determine whether sample richness was even enough for standard analysis across depths, the large pyrosequencing dataset was analyzed for Chao1 indices, which estimated total observable species. There was no significant depth-related trend (Fig. S1), so comparisons across depths may be interpreted through diversity analyses with equal sampling effort, which was achieved through Qiime's *multiple_rarefactions.py* script as described above.

Nodules

Small nodules, thought to be the most recent and actively growing surfaces of microbialites, were taken from microbialites at similar depths (~20 m) and were classified by color as either purple or green, based on visual description (Brady *et al.*, 2010). These assemblages were expected to be simple microbial communities, and this was confirmed through molecular analysis with general bacteria primers. It was determined that the majority of the microbial communities comprising these nodules are phototrophs of the phylum *Cyanobacteria* (Fig. 2; Fig. S2). *Leptolyngbya* spp. were most abundant in green nodules, and *Tolypothrix* spp. were most abundant in purple nodules. Additional *Cyanobacteria* from unclassified families IV and XIII were present in lower abundances. *Leptolyngbya* species were present in both purple and green nodules. *Tolypothrix spp.* was only seen in purple nodules, suggesting that this species gave the purple nodules their color. There was a higher level of *Cyanobacteria* diversity observed in purple nodules. In Nod.2 and Nod.5, three species were observed and two species were seen in Nod.6. In Nod.7 and Nod.1, green nodules, only one species of *Cyanobacteria* was observed (Fig. 2). A Bray–Curtis dissimilarity matrix was constructed from the rarified dataset, and this was visualized via a MDS plot, overlaid with a cluster analysis. Green nodule and purple nodule groupings do not have distinct community structure (Fig. 3A).

Cyanobacteria-specific Sanger sequencing

Since *Cyanobacteria* were predominant in nodules when using general bacterial primers, *Cyanobacteria*-specific primers were used in the construction of clone colonies from a suite of samples of both microbialites and soft mats (Fig. 1). Nodule biomass was included with total microbia-

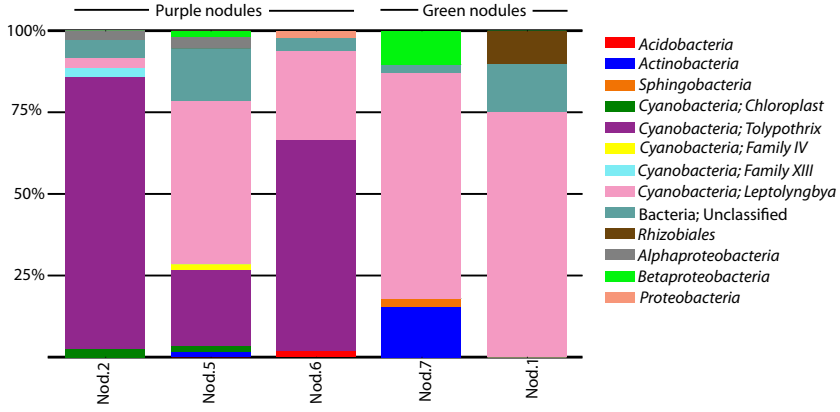

Fig. 2 Taxonomic profiles of nodule samples from the surface of Pavilion Lake microbialites, $N = 20$.

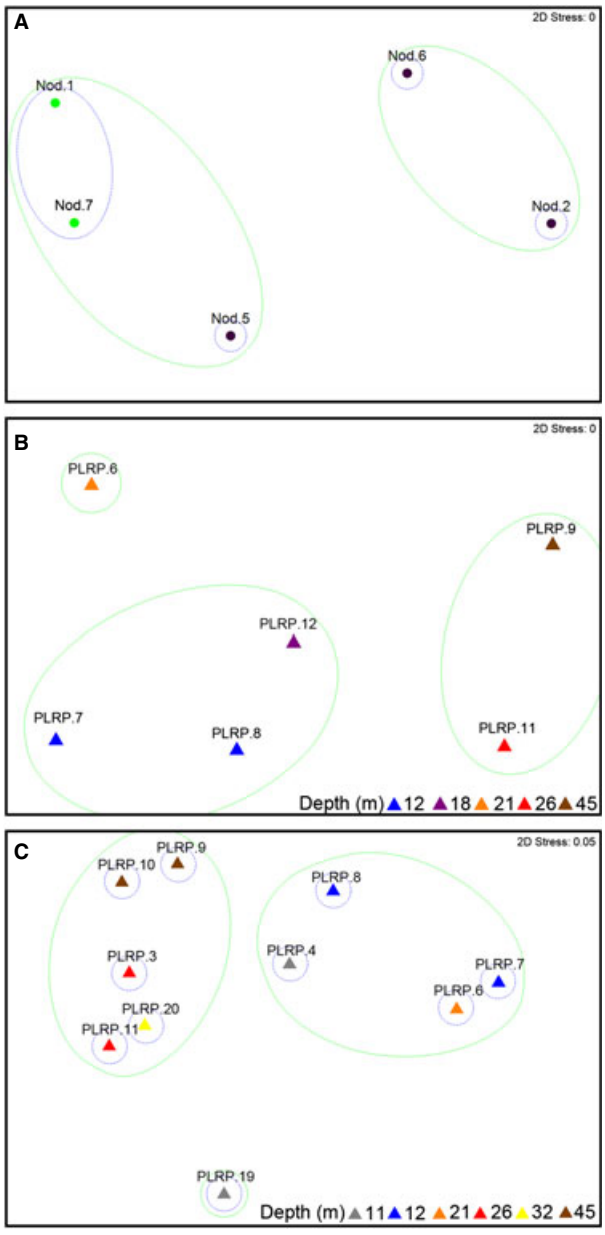

Fig. 3 Multidimensional scaling (MDS) ordination of rarified microbial communities. A) Sanger-sequenced nodules. Nodule type is indicated by purple or green color. B) Sanger sequencing of microbialites and soft mats with *Cyanobacteria*-specific primers, C) Pyrosequenced microbialite and soft mats with general bacteria primers ($N = 5900$). Legends show depth of sample in meters. For all panels, community similarity of 40% is indicated by a blue line, 20% by a green line.

lite samples as they were not separated from the microbialite surface community in this analysis. Despite the small dataset of 12 sequences per sample, differences in diversity can already be seen. Microbialites from 12 to 18 meters have a more diverse phototroph population with an average of 4.3 orders per sample, compared to deeper microbialites (21–45 m) and soft mats which average 2.2 orders per sample (Fig. 4). Five of the seven most abundant OTUs were seen only above 21 meters depth, but the two most abundant OTUs were seen in all samples, although present at a higher abundance at depth. Abundant OTUs group with *Leptolyngbya* and *Tolypothrix* species (Fig. 5). Many close relatives come from polar dry valleys as well as other carbonate-precipitating environments such as tufa-forming biofilms, alkaline thermal springs, and other microbialite systems (Table 2).

The relationships between detected taxa were investigated for depth-dependent trends using OTU-level comparisons (97% sequence similarity groupings), which are more discriminating than the taxonomy levels previously shown (Fig. 4). Soft mats were very distinct from lithifying microbialites (data not shown), and these samples were removed from further analysis. With mats excluded, a distinction between communities ≤21 m and ≥26 m depth can be seen for microbialite samples. Samples ≤21 m grouped together at the 20% similarity threshold, with only PLRP.6 as an outlier and the 26 m and 45 m samples clustered together at 20% similarity (Fig. 3B).

Total community analysis via pyrosequencing

To more robustly test whether the microbial communities of Pavilion Lake microbialites show distinct patterns with depth, a high-throughput analysis of the total bacterial community was performed. After extensive quality trimming and denoising, a total of 162 237 sequences were generated from 13 samples: 10 microbialites and three soft mats. These sequences were binned into OTUs at the 97% identity level. Diversity comparisons were done from a random subsampling of sequences from each sample ($n = 5900$ for microbialites and $n = 600$ for soft mats), and ten iterations of subsampling were generated. Taxonomy and sample similarity via MDS was calculated for each iteration. Conclusions were the same across all iterations, so only the first iteration is discussed.

Soft Mats

Cyanobacteria were shown to be abundant across all samples (Fig. 6). Noticeable exceptions with low *Cyanobacteria* abundance included soft mat sample PLRP.16, as well as a deep microbialite sample (PLRP.10) that had failed in the Sanger-sequencing analysis. The most abundant OTUs from soft mat samples included *Beta-, Delta-, and Gammaproteobacteria, Flavobacteria,* and *Cyanobacteria* (Table 2). Of the top 50 most abundant OTUs for microbialites and soft mats, only six were shared (Fig. S3). Soft mats clustered separate from microbialite samples by MDS, indicating large differences between these communities (data not shown). To investigate depth-related trends, only microbialite samples were used for further analysis.

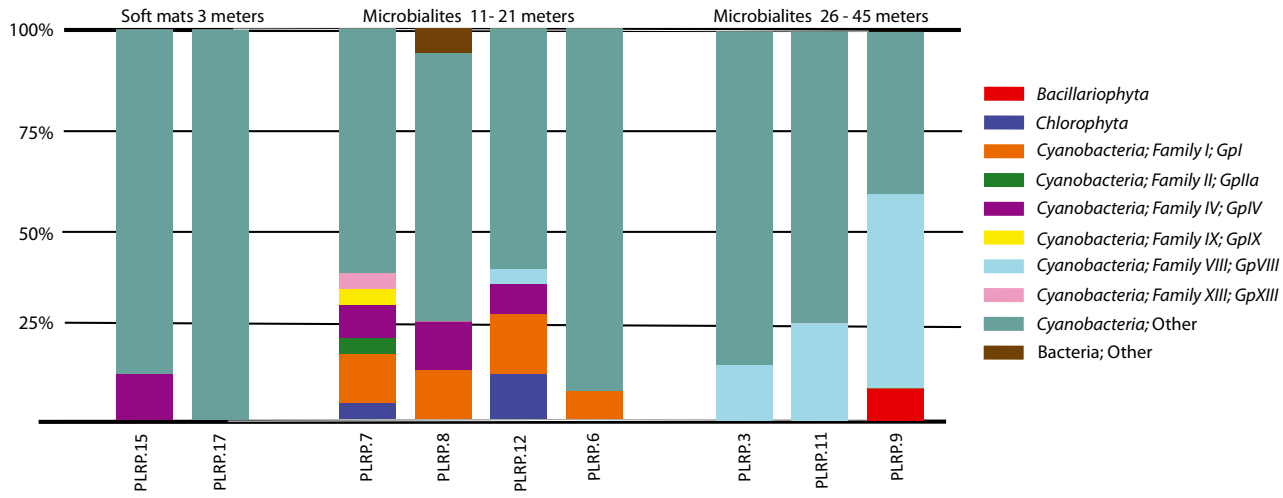

Fig. 4 Taxonomic profiles of microbialite and soft mat samples from Sanger sequencing with primers targeting *Cyanobacteria* (Cya359F, Cya781R). *N* = 12.

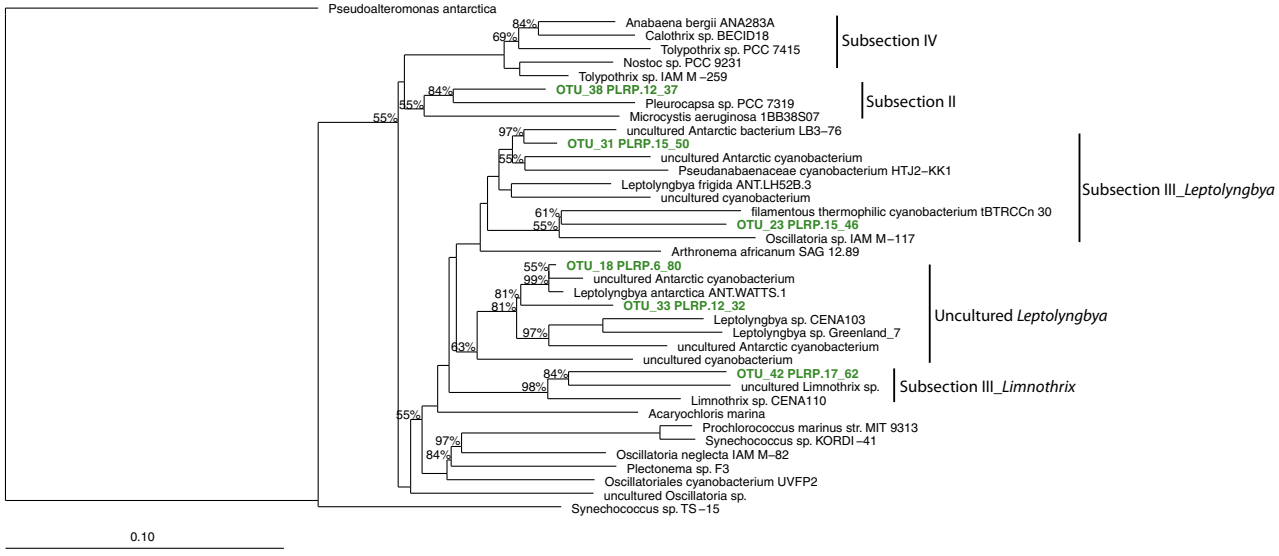

Fig. 5 Phylogenetic tree of abundant operational taxonomic units (OTUs) (green) from Sanger sequencing of microbialites with *Cyanobacteria*-specific primers, constructed using neighbor-joining method with 1000 bootstrap replicates. Bootstrap values over 50% are shown.

Microbialites

Visualizing the total microbialite bacterial community, two distinct clusters were observed at 20% similarity. Samples ≤21 m group together and samples ≥26 m grouped together, similar to the trend noted in the cyanobacterial analysis (Fig. 3C). One sample from 11 m (PLRP.19) was an outlier to these groups. To determine the strength of depth associations observed, data were compared to a model matrix for the depth categories of ≤21 and ≥26 m, based on the *Cyanobacteria* dataset, the pyrosequenced total community dataset, and various subsets of the pyrosequenced data (Table 3). Observed differences in the microbial community above and below ~25 m indicate a true structure between the communities (Table 3).

Microbialites from 11 to 21 m depth had, on average, 33.4% of sequences related to *Cyanobacteria*, whereas 26 m and below had an average of 19.2%. On deeper microbialites, *Acidobacteria*, *Nitrospira*, and *Proteobacteria* were more abundant (Fig. 6). The majority of *Acidobacteria*-related OTUs are closely related to *Candidatus Chloroacidobacterium thermophilum*, a recently characterized photoheterotrophic member of the phylum (Bryant *et al.*, 2007; Fig. S2). The top 21 OTUs included, in decreasing order, *Cyanobacteria*, *Proteobacteria*, *Nitrospirae*, and *Acidobacterium* (Table 2). Based on SIMPER analysis, the five most influential OTUs for depth category separation were all *Cyanobacteria*-related and account for 22.6% of the dissimilarity between depth categories (Table 3). OTUs

Table 2 Abundant operational taxonomic unit (OTU) information, taxonomy, and environment associations

Dataset	Most abundant OTUs	Number of Sequences ≤21 m	Number of Sequences ≥26 m	Total sequences per OTU	Taxonomy (BLAST consensus)	Environments previously found in
Pyrosequencing – microbialite biomass – general bacteria primers	OTU-11402	310	1337	1647	*Cyanobacteria*	Pavilion lake, Antarctic dry valleys, *Cyanobacteria* mats
	OTU-11111	1230	355	1585	*Cyanobacteria*	Pavilion lake, tufa-forming biofilms, Atacama desert
	OTU-2663	1050	108	1158	*Tolypothrix*	Pavilion lake, Deeply buried coral carbonates in marine sediment, Antarctic dry valleys
	OTU-11499	331	736	1067	*Nitrospirales*	Tufa-forming biofilms
	OTU-2187	56	794	850	*Cyanobacteria*	Highborne Cay microbialites, sandy carbonate sediment, Antarctic dry valleys
	OTU-1961	948	2	950	*Cyanobacteria*	Antarctic dry valleys, high Arctic snow, permafrost
	OTU-12633	725	13	738	*Lysobacter*	Tufa-forming biofilms
	OTU-10835	583	24	607	*Cyanobacteria*	Antarctic dry valleys, *Cyanobacteria* mats (McMurdo Ice Shelf)
	OTU-5091	478	98	576	*Cyanobacteria*	*Cyanobacteria* mats (McMurdo Ice Shelf), arid polar deserts, Antarctic dry valleys
	OTU-9048	77	450	527	*Rhizobiales*	Biofilms in karst aquifers, tufa-forming biofilms, glacial sediment
	OTU-11336	197	317	514	*Alphaproteobacteria*	Soil microbial communities, tufa-forming biofilms
	OTU-7552	202	267	469	*Nitrospira*	Glacier sediment, tufa-forming biofilms
	OTU-9779	368	5	373	*Cyanobacteria*	Antarctic dry valleys, high Arctic freshwater sediments
	OTU-8622	302	45	347	*Alphaproteobacteria*	Tufa-forming biofims, sewer sludge
	OTU-11510	56	260	316	*Acidobacteria*	Tufa-forming biofilms, petroleum-contaminated Arctic soils
	OTU-7374	95	210	305	Uncultured bacteria	Rice paddy soil, geothermal spring
	OTU-9981	57	258	315	*Cyanobacteria*	Coastal marine water column, hot spring biofilm (Izmir, Turkey)
	OTU-9400	1	324	325	*Cyanobacteria*	Microbial mats in rivers and geothermal settings
	OTU-11296	123	187	310	*Cyanobacteria*	Pavilion lake, Antarctic meltwater microbial mats
	OTU-2606	96	208	304	*Nitrospira*	Carbonate caves, tufa core samples
	OTU-11607	289	0	289	*Cyanobacteria*	Highborne Cay microbialites, Ruidera pools microbialites
Sanger microbialite biomass – *Cyanobacteria* primers	OTU-1	3	8	11	Uncult. *Cyanobacterium*	Pavilion lake, Antarctic dry valleys, alkaline thermal springs (Yellowstone National Park, USA)
	OTU-38	1	9	10	Uncult. *Cyanobacterium*	Mangrove swamps, microbialites (Lake Alchichica, Mexico)
	OTU-18	8	0	8	*Leptolyngbya* sp.	Sulfur spring, Taylor valley (Antarctica), high Arctic desert
	OTU-31	7	0	7	Uncultured	Glacial snow (Tibetan Plateau), Antarctic dry valleys,
	OTU-23	5	0	5	Uncult. *Cyanobacterium*	Sulfur spring (Lake Erie, Michigan, USA), tufa-forming biofilms
	OTU-42	4	0	4	Uncult. *Cyanobacterium*	Sulfur spring (Lake Erie, Michigan, USA)
	OTU-33	3	0	3	Uncult. *Cyanobacterium*	McMurdo dry valleys (Antarctica)
Sanger nodule biomass – general bacteria primers	OTU-0	0	41	41	*Tolypothrix* sp.	Pavilion lake, coral carbonate deposits in marine sediment, recently deglaciated soils
	OTU-35	26	13	39	*Leptolyngbya* sp.	Antarctic dry valleys, benthic *Cyanobacteria* mats in the high Arctic

Table 2 (continued)

Dataset	Most abundant OTUs	Number of Sequences ≤21 m	Number of Sequences ≥26 m	Total sequences per OTU	Taxonomy (BLAST consensus)	Environments previously found in
	OTU-5	0	17	17	*Tolypothrix* sp.	Pavilion lake, coral carbonate deposits in marine sediment, recently deglaciated soils
	OTU-9	12	3	15	Uncult. *Cyanobacterium*	Benthic *Cyanobacteria* mats in the high Arctic and Antarctic,
	OTU-14	0	8	8	*Leptolyngbya* sp.	Pavilion lake, quartz hypoliths
	OTU-6	0	6	6	Uncult. *Cyanobacterium*	Pavilion Lake, tufa-forming biofilms
	OTU-15	0	5	5	*Tolypothrix* sp.	Pavilion Lake, coral carbonate deposits in marine sediment, recently deglaciated soils

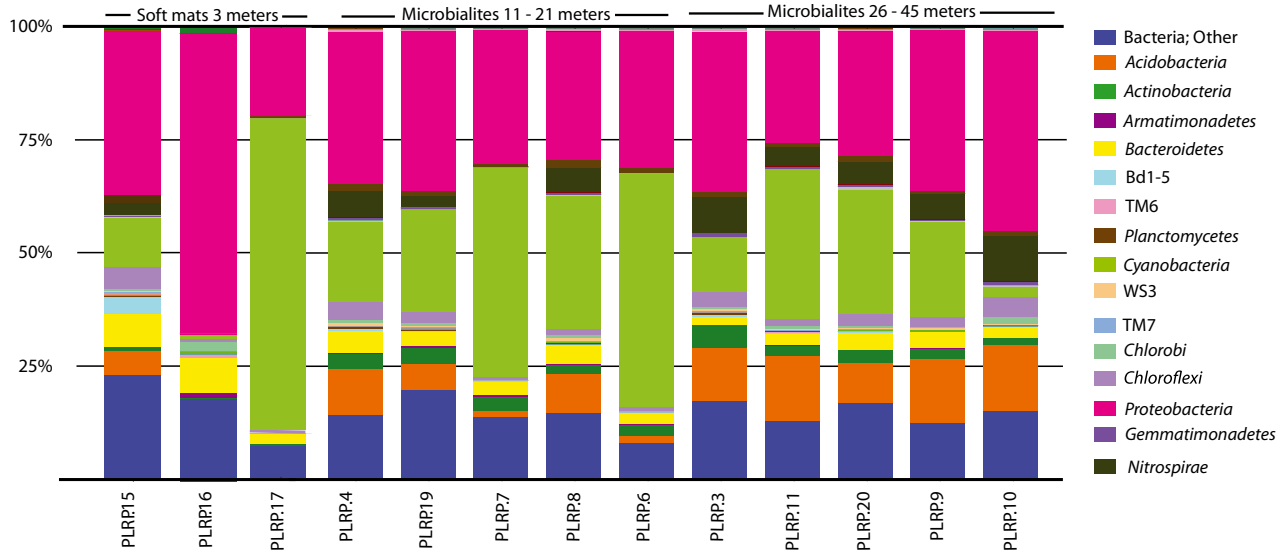

Fig. 6 Taxonomic profiles of microbialite and soft mat samples from pyrosequencing with general bacteria primers (B27F/B338R). $N = 5900$ for microbialites, $N = 600$ for soft mats.

grouped into a phylum level abundance were also compared, and again, *Cyanobacteria* were observed to have the largest effect on depth category dissimilarity (28.7%). The second most important phylum for between-group dissimilarity is *Acidobacteria* (20.9%), and as mentioned, most acidobacterial OTUs clustered with a known photoheterotroph (Table 3, Fig. S2).

$\delta^{13}C$ Isotopes

The effect of these phototrophs was seen in the overall carbonate isotopic values. In general, the majority of the $\delta^{13}C_{carb}$ values for the microbialite samples included in this study fall within the predicted equilibrium range of −1.2 to 1.1‰ (Fig. 7). Notable exceptions were two of the microbialites recovered from 11 m with $\delta^{13}C_{carb}$ values that were above the predicted range indicating a predominantly phototrophic influence on carbonate precipitation at this depth. Microbialites recovered from below 11 m fall within the equilibrium range; however, a statistically significant distinction is noted between samples from the upper two depths of 11 and 18 m and deeper samples from 26 and 45 m as samples from the two deepest depths demonstrate more ^{13}C-depleted $\delta^{13}C_{carb}$ values (paired t test, $P = 0.0033$).

DISCUSSION

In this study, the microbial diversity of Pavilion Lake microbialites, soft mats, and nodules was examined through multiple molecular methods. Support for a phototrophic community in the nodules was found, confirming previous

Table 3 Results of statistical tests

Resemblance matrix	Rho	*P*-value
RELATE test*		
Cyanobacteria, Sanger sequencing	0.29	0.2
All bacteria, pyrosequencing	0.54	0.009
Cyanobacteria subtracted, pyrosequencing	0.44	0.009
Cyanobacteria only, pyrosequencing	0.64	0.007
Cyanobacteria and *Acidobacteria*, pyrosequencing	0.66	0.009

Resemblance matrix	Highest contribution to ≤21 m within-group similarity†	Highest contribution to ≥26 m within-group similarity†	Highest contribution to between-group dissimilarity (%)
SIMPER test			
Top 60 most abundant operational taxonomic units (OTUs)	OTU-1111 (8.7) (14.9)	OTU-11499 (7.5) (12.7)	OTU-11111 (4.4)
	OTU-2663 (7.6) (13.9)	OTU-2187 (4.8) (11.9)	OTU-11402 (4.2)
	OTU-5091 (6.1) (9.6)	OTU-11336 (4.8) (8.1)	OTU-1961 (4.0)
	OTU-10835 (5.0) (9.9)	OTU-9048 (4.5) (9.1)	OTU-2187 (3.6)
	OTU-1961 (4.7) (11.8)	OTU-11510 (4.2) (7.1)	OTU-2663 (3.4)
Phylum abundance	*Proteobacteria* (26.8) (43.0)	*Proteobacteria* (24.2)(44.2)	*Cyanobacteria* (28.7)
	Cyanobacteria (24.2) (43.5)	Bacteria;Other (16.8) (30.0)	*Acidobacteria* (20.9)
	Bacteria;Other (16.9) (28.9)	*Acidobacteria* (15.2) (27.3)	*Nitrospirae* (18.7)
	Bacteroidetes (8.4) (14.3)	*Cyanobacteria* (13.9) (31.6)	*Proteobacteria* (8.0)
	Actinobacteria (7.8) (13.1)	*Nitrospirae* (10.2) (19.4)	*Chloroflexi* (7.7)
	Acidobacteria (7.7) (16.6)	*Bacteroidetes* (6.8) (12.7)	Bacteria;Other (6.9)

*Results are considered significant when $\rho > 0.5$ and $P \leq 0.01$.†First number indicates percent contribution to within-group similarity, second number is the percentage abundance within group.

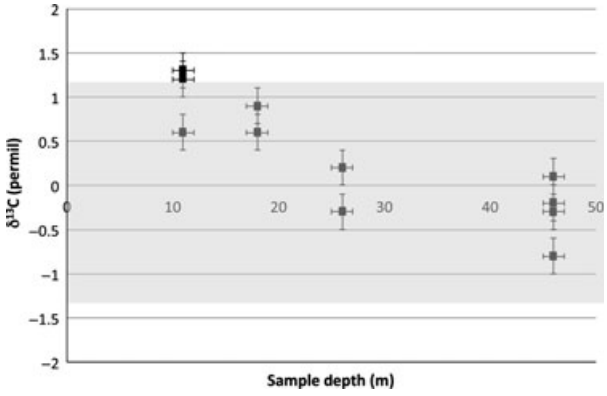

Fig. 7 $\delta^{13}C_{carbonate}$ for replicate analysis for each of the target depths. The shaded area shows the range of values expected for abiotic equilibrium precipitation (−1.2 to 1.1‰). In general, the isotopic compositions of the carbonate from the microbialites fall within the range predicted for equilibrium precipitation from lake water dissolved inorganic carbon (DIC).

isotopic and microscopic analyses (Fig. 2, Brady *et al.*, 2010; Laval *et al.*, 2000). *Tolypothrix*, the most abundant genus found in purple nodules, is known for complementary chromatic adaptation (CCA): the ability to adjust pigment usage to available light regimes (Bennet and Bogorad 1973). Its red-shifted pigments likely contribute to the color of these nodules and also may allow for the expanded diversity of *Cyanobacteria* within the nodules, due to their removal from competition for shorter wavelengths of light. *Leptolyngbya* species were present in purple nodules and were also the dominant genus in green nodules. Similar *Cyanobacteria* groups were seen in the nodules and in total microbialite community, showing that the nodular, small growth structures are well related to the larger microbialite (Table 2). However, these data are not enough to explain the process of nodules becoming larger microbialite structures.

Very little overlap was seen between soft mat and lithifying microbialite *Cyanobacteria* populations. Of shared OTUs, only one is *Cyanobacteria*-related (OTU-5406); it is the second most abundant OTU amongs soft mat samples, but the 45th most abundant OTU amongs microbialite samples. This suggests that some species of *Cyanobacteria* may not be a key component to the lithification process (Fig. S3). *Oscillatoriales* spp. were a numerically dominant member of all Pavilion Lake microbialites, yet different OTUs within this order dominated at different depths (Table 2, Fig. S2). Interestingly, *Pleurocapsales* spp. became more abundant in the deeper ≥26 m microbialites of Pavilion Lake (Table 2, Fig. S2), a phenomenon previously noted in microbialites of Lake Alchichica (Couradeau *et al.*, 2011). Members of subsection-III within the phylum *Cyanobacteria* were the most abundant in microbialites above 25 m, particularly sequences that cluster with the species *Leptolyngbya frigida* and *Leptolyngbya antarctica* (Figs S2, S3). Given the high abundance of *L. frigida* and *L. antarctica* in the pyrosequencing dataset, it was expected that these would match with sequences from the Sanger-sequenced *Cyanobacteria*-specific dataset as

well as the general bacteria investigation of the nodules. Indeed, the most abundant OTUs from all sequencing efforts clustered closely with these species (Fig. 5, Fig. S2).

Many of the OTUs detected in this study cluster closely with species previously observed in polar settings (Fig. 5, Taton *et al.* 2006). It has been shown that some benthic microbial mats in Antarctic lakes do form lithifying structures (Parker *et al.*, 1981; Wharton *et al.*, 1983; Andersen *et al.*, 2011). The microbial communities of microbialite growths in these polar lakes are poorly characterized. However, it is clear that they share common microbial consortia with those of Pavilion Lake, as well as characteristics in their growth environment (low PAR, oligotrophy, low sedimentation, depth gradients, temperature). Further study of these polar microbialites with advanced molecular tools, as well as continued investigations of Pavilion Lake's structures with RNA-based and metagenomic analyses, will clarify microbialite accretion mechanisms in dynamic growth environments that do not resemble 'typical' microbialite habitats in shallow pools and marginal reefs.

Beyond *Cyanobacteria*, other phototrophs were detected in Pavilion Lake microbialites. *Acidobacteria* was an abundant member phylum of these structures, particularly in the ≥26 m depth category (Fig. 6). Additionally, it was the second most responsible phylum for differences in community above and below 25 m (contributing 20.9% between-group dissimilarity), just past *Cyanobacteria* (Table 3). The most abundant OTU associated with *Acidobacteria*, OTU-11510, exhibited a distinct preference for depths ≥26 m, and phylogenetic analysis showed it is closely related to the recently characterized photoheterotrophic member of the *Acidobacteria* phylum, *Candidatus Chloracidobacterium thermophilum* (Table 2, Fig. S2). Other OTUs identified as *Candidatus Chloracidobacterium* (OTU-3943 and OTU-170) were prevalent at depth and not seen in the ≤21 m depth category. *Candidatus C. thermophilum* exhibits a bacteriochlorophyll profile and the *csmA* gene that is integral to the construction of chlorosomes, very similar to phototrophic members of *Chloroflexi* and *Chlorobi* (Bryant *et al.*, 2007). Chlorosomes are thought to enable organisms to harvest light at low PAR (Garcia Costas *et al.*, 2012). The use of chlorosomes may allow the maintenance of phototrophic activity in deep microbialites. OTUs associated with *Chlorobi* and *Chloroflexi* were not very abundant overall (0.5% and 2.4% of total sequence abundance, respectively), suggesting deep microbialites may be a niche environment for *Candidatus C. thermophilum* where it is able to out compete similarly functioning microbes. Other genera that include known phototrophs were detected through pyrosequencing including all phototrophic members of the *Alphaproteobacteria* (*Rhodobacteraceae* sp., *Hyphomicrobiaceae* sp., *Sphingomonadales* sp., and *Rhodospirillales* sp.). *Alphaproteobacteria* accounted for 15.0% of all sequence data compared to 12.9% for *Beta-*, *Delta-*, and *Gammaproteobacteria* combined. With depth, *Alphaproteobacteria* were evenly distributed accounting for an average of 15% of the total community. This suggests a ubiquitous background community of *Proteobacteria*-associated photoheterotrophs (primarily purple non-sulfur bacteria and green sulfur bacteria). Similar distributions of *Alphaproteobacteria*, *Chlorobi*, and *Chloroflexi* have been seen in other microbialite systems; however, *Chloroacidobacteria* have not been previously noted (Breitbart *et al.* 2009, Couradeau *et al.*, 2011; Foster & Green, 2011; Khodadad & Foster, 2012).

In microbial mats, most often anoxygenic photoheterotrophs are sustained with a steady flux of electron donors like sulfide from other anoxic metabolisms such as sulfate reduction occurring deeper in the mat (Visscher *et al.*, 1998; Papineau *et al.*, 2005). Most sulfate reducers are found in the *Deltaproteobacteria*; additionally, some *Firmicutes*, *Nitrospirae*, and Archaea are known for this metabolism (Loy *et al.*, 2002; Muyzer & Stams, 2008). Of these, we did not survey Archaea, *Firmicutes* made up <0.1% of the data, and observed *Nitrospirae* did not group with known sulfate reducers from the phylum (Fig. S2). *Deltaproteobacteria* made up 3.8% of total sequence abundance in microbialites. Previous research has indicated an important role for sulfate reduction in microbialite formation (Visscher *et al.*, 2000; Visscher & Stolz, 2005; Havemann & Foster, 2008; Breitbart *et al.*, 2009; Baumgartner *et al.*, 2009; Foster & Green, 2011; Mobberley *et al.* 2012). While the even distribution of sulfate-reducing bacteria across depths implicates them as an important member of microbialite accretion, it also indicates they are not associated with particular morphologies.

Planctomycetes spp. have also been determined to be a dominant and critical member of many other microbialite systems (Burns *et al.*, 2004; Havemann & Foster, 2008; Baumgartner *et al.*, 2009; Breitbart *et al.*, 2009; Foster & Green, 2011); however, this phylum was conspicuously absent from Pavilion Lake microbialites, representing only 1.1% of sequence abundance in the pyrosequencing dataset. This could reflect issues of primer bias rather than a true absence from the community as the reverse primer matched well with less than half of all clades within the phylum, based on comparisons to the SILVA database.

Previous analysis of Pavilion Lake chemistry has shown two noticeable characteristics at depth (i.e., >25 m); a lower total nitrogen to total phosphorous ratio (TN:TP) by a factor of 2 relative to the shallows, and a higher calcite saturation index ($\Delta SI_{calcite}$) at depth, facilitating easier carbonate precipitation (Lim *et al.*, 2009). As nitrogen availability for microbes changes with depth, the microbial community may be responding. *Nitrospirae spp.* exhibited a higher abundance in the ≥26 m depth category and was the third most responsible for the difference in depth categories, contributing 18.7% of between-group dissimilarity

(Table 3). This phylum is known for nitrite-oxidizing bacteria (Garrity & Holt, 2001). The most abundant *Nitrospirae* OTUs in Pavilion Lake microbialites are related to a known chemolithoautotrophic nitrite oxidizer, *Nitrospira moscoviensis* (Fig. S2, Ehrich *et al.*, 1995). This suggests deep microbialites may have more biologically produced nitrate (NO_3^-) available. Additionally, a higher specific conductance at depth indicates that groundwater of a higher salinity than the lake water is entering the lake basin through unidentified conduits, flowing down the sides, and pooling at the bottom (Lim *et al.*, 2009). This groundwater may bring additional nutrients and metals that benefit populations at depth more than shallow structures, compensating for lower PAR and determining community composition, although this cannot be proven with the available datasets.

In Pavilion Lake, despite changes in PAR with depth (Laval *et al.*, 2000; Lim *et al.*, 2009), little change was seen for overall richness estimates (Fig. S1). Changes in community did not occur along a continuous gradient (Figs 3 and 4); instead, distinct depth categories (≤21 and ≥26 m) were seen through statistical analysis of these data (Fig. 3B, C, Table 3). Phototroph-associated OTUs were the elements driving these community depth categories; predominantly *Cyanobacteria* and sequences clustering with the recently characterized *Chloracidobacterium* (Table 3, Bryant *et al.*, 2007). The two shallow depth microbialites (11 m) exhibited $\delta^{13}C_{carb}$ values that lie above the abiotic range, indicating that phototrophic influence affected carbonate precipitation in these samples. While the remaining samples fell within the equilibrium range (Fig. 7) and abiotic processes cannot be ruled out, there is a statistically significant distinction between the upper two depths (11 and 18 m) and the more ^{13}C-depleted deeper samples (26 and 45 m). Although the relative ^{13}C-enrichment of the shallower depths cannot be assigned unequivocally to photosynthetic activity, it is possible that the trend toward lower $\delta^{13}C_{carb}$ values with increasing depth reflects a greater contribution of ^{13}C-depleted heterotrophic inputs. Increased heterotrophic inputs may mask any photosynthetically induced ^{13}C-enrichments at these deeper depths. A shift toward increased heterotrophy-derived DIC is consistent with the observed shift in microbial community toward a greater heterotrophic abundance.

This study implicates light as an important factor for microbial communities on microbialites across depths in the lake. In the shallows, the presumed photoautotrophs of *Cyanobacteria* are the population responsible for the shallow depth category. The presumed photoheterotrophs of *Chloroacidobacterium* drive the formation of the deeper category. In fact, using just these two populations, the model of distinct community change happening between 21 and 26 m is best supported (Table 3). Thus, it appears that the most fundamental dichotomy between the ≤21 and ≥26 m depth categories is not phototroph vs. non-phototroph, but autotroph vs. heterotroph. Despite the knowledge of the microbial diversity of the Pavilion Lake microbialites, nodules and soft mats presented here, there is little indication that particular individuals or groups of bacterial species dictate microbialite morphology. These data show that classes of photoautotrophy and photoheterotrophy may be important factors in microbialite development, allowing light to maintain an overall control on the formation of modern-day microbialites.

It is important to note that this work is not meant to definitively determine the acting mechanisms behind microbialite accretion and morphology diversification. Contrary to our hypothesis, microbial diversity did not correspond to microbialite morphology, leaving room for further hypothesis testing to determine mechanistic changes in carbonate deposition. Represented here is a detailed survey of microbial diversity from the only microbialite growth system known to span such a wide depth range: a system that holds much potential in the search for knowledge on life's earliest origins.

ACKNOWLEDGMENTS

Special thanks to Donnie Reid and all members of the PLRP field team, especially the science divers and deep worker pilots who collected the samples. We thank Jennifer Hansen for laboratory assistance with carbonate measurements. This work was supported by the NASA Moon and Mars Analog Mission Activities (MMAMA) grant to D. Lim, the Canadian Space Agency's (CSA) Canadian Analogue Research Network (CARN), and Analogue Missions programs, Nuytco Research, the Delaware Space Grant Consortium funded by NASA CAN NNX10AN63H to D. Mullan and by the UD College of Earth, Ocean, and Environment. J. Russell was supported by a Marian R. Okie Fellowship. This publication was made possible by the National Science Foundation EPSCoR Grant No. EPS-0814251 and the State of Delaware. We are also grateful to Linda and Mickey Macri for hosting the PLRP project from 2004 to present and to the Ts'Kw'aylaxw First Nation and British Columbia Parks for their continued support of our research. This is Pavilion Lake Research Project publication #13-02.

REFERENCES

Abed RM, Golubic S, Garcia-Pichel F, Camoin GF, Sprachta S (2003) Characterization of microbialite-forming Cyanobacteria in a tropical lagoon: Tikehau Atoll, Tuamotu, French Polynesia. *Journal of Phycology* **39**, 862–873.

Allen MA, Goh F, Burns BP, Neilan BA (2009) Bacterial, archaeal and eukaryotic diversity of smooth and pustular microbial mat

communities in the hypersaline lagoon of Shark Bay. *Geobiology* **7**, 82–96.
Altermann W, Kazmierczak J, Oren A, Wright DT (2006) Cyanobacterial calcification and its rock-building potential during 3.5 billion years of Earth history. *Geobiology* **4**, 147–166.
Altschul SF, Gish W, Miller W, Myers EW, Lipman DJ (1990) Basic local alignment search tool. *Journal of Molecular Biology* **215**, 403–410.
Andersen DT, Sumner DY, Hawes I, Webster-Brown J, McKay CP (2011) Discovery of large conical stromatolites in Lake Untersee, Antarctica. *Geobiology* **9**, 280–293.
Andres MS, Sumner DY, Reid RP, Swart PK (2006) Isotopic fingerprints of microbial respiration in aragonite from Bahamian stromatolites. *Geology* **34**, 973–976.
Arp G, Thiel V, Reimer A, Michaelis W, Reitner J (1999) Biofilm exopolymers control microbialite formation at thermal springs discharging into the alkaline Pyramid Lake, Nevada, USA. *Sedimentary Geology* **126**, 159–176.
Baumgartner LK, Reid RP, Dupraz C, Decho AW, Buckley DH, Spear JR, Przekop KM, Visscher PT (2006) Sulfate reducing bacteria in microbial mats: changing paradigms, new discoveries. *Sedimentary Geology* **185**, 131–145.
Baumgartner LK, Spear JR, Buckley DH, Pace NR, Reid RP, Dupraz C, Visscher PT (2009) Microbial diversity in modern marine stromatolites, Highborne Cay, Bahamas. *Environmental Microbiology* **11**, 2710–2719.
Bennett A, Bogorad L (1973) Complementary chromatic adaptation in a filamentous blue-green alga. *Journal of Cell Biology* **58**, 419–35.
Bonilla- Rosso G, Peimbert M, Alcaraz LD, Hernandez I, Eguiarte LE, Olmedo-Alvarez G, Souza V (2012) Comparative metagenomics of two microbial mats at Cuatro Cienegas Basin II: community structure and composition in oligotrophic environments. *Astrobiology* **12**, 659–673.
Brady AL, Slater G, Laval B, Lim DS (2009) Constraining carbon sources and growth rates of freshwater microbialites in Pavilion Lake using ^{14}C analysis. *Geobiology* **7**, 544–555.
Brady AL, Slater GF, Omelon CR, Southam G, Druschel G, Andersen DT, Hawes I, Laval B, Lim DSS (2010) Photosynthetic isotope biosignatures in laminated micro-stromatolitic and non-laminated nodules associated with modern, freshwater microbialites in Pavilion Lake, B.C. *Chemical Geology* **274**, 56–67.
Breitbart M, Hoare A, Nitti A, Siefert J, Haynes M, Dinsdale E, Edwards R, Souza V, Rohwer F, Hollander d. (2009) Metagenomic and stable isotopic analyses of modern freshwater microbialites in Cuatro Ciénegas, Mexico. *Environmental Microbiology* **11**, 16–34.
Bryant DA, Costas AMG, Maresca JA, Chew AGM, Klatt CG, Bateson MM, Tallon LJ, Hostetler J, Nelson WC, Heidelberg JF, Ward DM. (2007) Candidatus Chloracidobacterium thermophilum: an aerobic phototrophic Acidobacterium. *Science (New York, NY)* **317**, 523–526.
Burne RV, Moore LS (1987) Microbialites: organosedimentary deposits of benthic microbial communities. *Palaios* **2**, 241–254.
Burns BP, Goh F, Allen M, Neilan BA (2004) Microbial diversity of extant stromatolites in the hypersaline marine environment of Shark Bay, Australia. *Environmental Microbiology* **6**, 1096–1101.
Caporaso JG, Kuczynski J, Stombaugh J, Bittinger K, Bushman FD, Costello EK, Fierer N, Peña AG, Goodrich JK, Gordon JI, Huttley GA, Kelley ST, Knights D, Koenig JE, Ley RE, Lozupone CA, McDonald D, Muegge BD, Pirrung M, Reeder J, Sevinsky JR, Turnbaugh PJ, Walters WA, Widmann J, Yatsunenko T, Zaneveld J, Knight R. (2010) QIIME allows analysis of high- throughput community sequencing data. *Nature Publishing Group* **7**, 335–336.
Clarke KR, Gorley RN (2006) *PRIMER v6: User Manual/ Tutorial.* Primer-E, Plymouth, UK.
Couradeau E, Benzerara K, Moreira D, Gérard E, Kaźmierczak J, Tavera R, López-García P (2011) Prokaryotic and eukaryotic community structure in field and cultured microbialites from the alkaline Lake Alchichica (Mexico). *PLoS ONE* **6**, e28767.
Decho AW (1990) Microbial exopolymer secretions in ocean environments: their role(s) in food webs and marine processes. *Oceanography and Marine Biology: An Annual Review* **28**, 73–153.
Dupraz C, Visscher PT (2005) Microbial lithification in marine stromatolites and hypersaline mats. *Trends in microbiology* **13**, 429–438.
Dupraz C, Reid RP, Braissant O, Decho AW, Norman RS, Visscher PT (2009) Processes of carbonate precipitation in modern microbial mats. *Earth-Science Reviews* **96**, 141–162.
Ehrich S, Behrens D, Lebedeva E, Ludwig W, Bock E (1995) A new obligately chemolithoautotrophic, nitrite-oxidizing bacterium, Nitrospira moscoviensis sp. nov. and its phylogenetic relationship. *Archives of Microbiology* **164**, 16–23.
Foster JS, Green SJ (2011) Microbial diversity in modern marine stromatolites. In *Cellular Origin, Life in Extreme Habitats and Astrobiology: Stromatolites.* (ed Tewari V). Springer, Berlin, pp. 385–405.
Foster JS, Green SJ, Ahrendt SR, Golubic S, Reid RP, Hetherington KL, Bebout L (2009) Molecular and morphological characterization of cyanobacterial diversity in the marine stromatolites of Highborne Cay, Bahamas. *ISME Journal* **3**, 573–587.
Garcia Costas AM, Tsukatani Y, Rijpstra WIC, Schouten S, Welander PV, Summons RE, Bryant D, a. (2012) Identification of the bacteriochlorophylls, carotenoids, quinones, lipids, and hopanoids of "Candidatus Chloracidobacterium thermophilum". *Journal of Bacteriology* **194**, 1158–1168.
Garrity GM, Holt JG (2001) Phylum BVIII. Nitrospirae phy. nov. In *Bergey's Manual of Systematic Bacteriology: The Archaea and the Deeply Branching and Phototrophic Bacteria*, (eds Boone DR, Castenholz RW, Garrity GM). Springer-Verlag, New York, NY, pp. 451–464.
Gischler E, Gibson MA, Oschmann W (2008) Giant Holocene freshwater microbialites, Laguna Bacalar, Quintana Roo, Mexico. *Sedimentology* **55**, 1293–1309.
Grotzinger JP, Knoll AH (1999) Stromatolites in Precambrian carbonates: evolutionary mileposts or environmental dipsticks? *Annual Reviews of Earth and Planetary Science* **27**, 313–358.
Havemann SA, Foster JS (2008) Comparative characterization of the microbial diversities of an artificial microbialite model and a natural stromatolite. *Applied and Environmental Microbiology* **74**, 7410–7421.
Hollander DJ, Mckenzie JA (1991) CO_2 control on carbon-isotope fractionation during aqueous photosynthesis: a paleo-pCO_2 barometer. *Geology* **19**, 929–932.
Khodadad CLM, Foster JS (2012) Metagenomic and metabolic profiling of nonlithifying and lithifying stromatolitic mats of Highborne Cay, The Bahamas. *PLoS ONE* **7**, e38229.
Lane DJ (1991) 16S/23S rRNA sequencing. In *Nucleic acid Techniques in Bacterial Systematics* (eds Stackebrandt E, Goodfellow M). John Wiley and Sons, New York, NY, pp. 115–175.
Laval B, Cady SL, Pollack JC, McKay CP, Bird JS, Grotzinger JP, Ford DC, Bohm HR. (2000) Modern freshwater microbialite analogues for ancient dendritic reef structures. *Nature* **407**, 626–629.

Lim DSS, Laval BE, Slater G, Antoniades D, Forrest AL, Pike W, Pieters R, Saffari M, Reid D, Schulze-Makuch D, Andersen D, McKay CP. (2009) Limnology of Pavilion Lake, B. C., Canada – Characterization of a microbialite forming environment. *Fundamental and Applied Limnology* **173**, 329–351.

Lim DSS, Brady AL, Pavilion Lake Research Project (PLRP) Team (Abercromby AF, Andersen DT, Andersen M, Arnold RR, Bird JS, Bohm HR, Booth L, Cady SL, Cardman Z, Chan AM, Chan O, Chénard C, Cowie BR, Davila A, Deans MC, Dearing W, Delaney M, Downs M, Fong T, Forrest A, Gernhardt ML, Gutsche JR, Hadfield C, Hamilton A, Hansen J, Hawes I, Heaton J, Imam Y, Laval BL, Lees D, Leoni L, Looper C, Love S, Marinova MM, McCombs D, McKay CP, Mireau B, Mullins G, Nebel SH, Nuytten P, Pendery R, Pike W, Pointing SB, Pollack J, Raineault N, Reay M, Reid D, Sallstedt T, Schulze-Makuch D, Seibert M, Shepard R, Slater GF, Stonehouse J, Sumner DY, Suttle CA, Trembanis A, Turse C, Wilhelm M, Wilkinson N, Williams D, Winget DM, Winter C. (2011) A historical overview of the Pavilion Lake Research Project - Analog science and exploration in an underwater environment. *Geological Society of America Special Papers* **483**, 85–115.

Lowe DR (1980) Stromatolites 3,400-Myr old from the Archean of Western Australia. *Nature* **284**, 441–443.

Loy A, Lehner A, Lee N, Adamczyk J, Meier H, Ernst J, Schleifer KH, Wagner M. (2002) Oligonucleotide microarray for 16S rRNA gene-based detection of all recognized lineages of sulfate-reducing prokaryotes in the environment. *Applied and Environmental Microbiology* **68**, 5064–5081.

Ludwig W, Strunk O, Westram R, Richter L, Meier H, Buchner A, Lai T, Steppi S, Jobb G, Förster W, Brettske I, Gerber S, Ginhart AW, Gross O, Grumann S, Hermann S, Jost R, König A, Liss T, Lüssmann R, May M, Nonhoff B, Reichel B, Strehlow R, Stamatakis A, Stuckmann N, Vilbig A, Lenke M, Ludwig T, Bode A, Schleifer KH. (2004) ARB: a software environment for sequence data. *Nucleic acids Research* **32**, 1363–1371.

Ludwig R, Al-Horani FA, de Beer D, Jonkers HM (2005) Photosynthesis-controlled calcification in a hypersaline microbial mat. *Limnology and Oceanography* **50**, 1836–1843.

Merz MUE (1992) The biology of carbonate precipitation by cyanobacteria. *Facies* **26**, 81–102.

Meyer M, Stenzel U, Myles S, Prüfer K, Hofreiter M (2007) Targeted high-throughput sequencing of tagged nucleic acid samples. *Nucleic acids Research* **35**, e97.

Mobberley JM, Ortega MC, Foster JS (2012) Comparative microbial diversity analyses of modern marine thrombolitic mats by barcoded pyrosequencing. *Environmental microbiology* **14**, 82–100.

Muyzer G, Stams AJM (2008) The ecology and biotechnology of sulphate-reducing bacteria. *Nature reviews. Microbiology* **6**, 441–454.

Nübel U, Garcia-Pichel F, Muyzer G (1997) PCR primers to amplify 16S rRNA genes from cyanobacteria. *Applied and Environment Microbiology* **63**, 3327–3332.

O'Leary MH (1988) Carbon isotope fractionation during photosynthesis. *BioScience* **38**, 328–336.

Papineau D, Walker JJ, Mojzsis SJ, Pace NR (2005) Composition and Structure of Microbial Communities from Stromatolites of Hamelin Pool in Shark Bay, Western Australia. *Applied and Environmental Microbiology* **71**, 4822–4832.

Parker BC, Simmons GM, Love FG, Wharton RA, Seaburg KG, Robert A (1981) Modern Stromatolites in Antarctic Dry Valley Lakes. *BioScience* **31**, 656–661.

Peimbert M, Alcaraz LD, Bonilla-Rosso G, Olmedo-Alvarez G, Garcia-Oliva F, Segovia L, Eguiarte LE, Souza V (2012) Comparative metagenomics of two microbial mats at Cuatro Cienegas Basin I: ancient lessons on how to cope with an environment under severe nutrient stress. *Astrobiology* **12**, 648–658.

Pinckney JL, Reid RP (1997) Productivity and community composition of stromatolitic microbial mats in the Exuma Cays, Bahamas. *Facies* **36**, 204–207.

Reid RP, Visscher PT, Decho AW, Stolz JF, Bebout BM, Dupraz C, Macintyre IG, Paerl HW, Pinckney JL, Prufert-Bebout L, Steppe TF, DesMarais DJ. (2000) The role of microbes in accretion, lamination and early lithification of modern marine stromatolites. *Nature* **406**, 989–992.

Revsbech NP, Jørgensen BB, Blackburn TH, Cohen Y (1983) Microelectrode studies of the photosynthesis and O2, H2S, and pH profiles of a microbial mat. *Limnology and Oceanography* **28**, 1062–1974.

Schloss PD, Westcott SL, Ryabin T, Hall JR, Hartmann M, Hollister EB, Lesniewski RA, Oakley BB, Parks DH, Robinson CJ, Sahl JW, Stres B, Thallinger GG, Van Horn DJ, Weber CF. (2009) Introducing mothur: open-source, platform-independent, community-supported software for describing and comparing microbial communities. *Applied and environmental microbiology* **75**, 7537–7541.

Schopf J, Packer B (1987) Early Archean (3.3-billion to 3.5-billion-year-old) microfossils from Warrawoona Group, Australia. *Science* **237**, 70–73.

Shiraiwa Y, Goyal A, Tolbert NE (1993) Alkalization of the medium by unicellular green algae during uptake of dissolved inorganic carbon. *Plant and Cell Physiology* **34**, 649–657.

Sumner DY (2001) Microbial influences on local carbon isotopic ratios and their preservation in carbonate. *Astrobiology* **1**, 57–70.

Taton A, Grubisic S, Balthasart P, Hodgson DA, Laybourn-Parry J, Wilmotte A (2006) Biogeographical distribution and ecological ranges of benthic cyanobacteria in East Antarctic lakes. *FEMS Microbiology Ecology* **57**, 272–289.

Thompson JB, Schultze-Lam S, Beveridge TJ, Des Marais DJ (1997) Whiting events: biogenic origin due to the photosynthetic activity of cyanobacterial picoplankton. *Limnology and Oceanography* **42**, 133–141.

Visscher PT, Stolz JF (2005) Microbial mats as bioreactors: populations, processes, and products. *Palaeogeography, Palaeoclimatology, Palaeoecology* **219**, 87–100.

Visscher PT, Reid RP, Bebout BM, Hoeft SE, Macintyre IG, Thompson JA Jr. (1998) Formation of lithified micritic laminae in modern marine stromatolites (Bahamas): the role of sulfur cycling. *American Mineralogist* **83**, 1482–1493.

Visscher PT, Reid RP, Bebout BM (2000) Microscale observations of sulfate reduction: correlation of microbial activity with lithified micritic laminae in modern marine stromatolites. *Geology* **28**, 919–922.

Wharton RA Jr, Parker BC, Simmons GM Jr (1983) Distribution, species composition and morphology of algal mats in Antarctic dry valley lakes. *Phycologia* **22**, 355–365.

SUPPORTING INFORMATION

Additional Supporting Information may be found in the online version of this article:

Fig. S1 Descriptions and diversity of sample set with depth. Sample type is coded by shape: triangles, microbialite samples; circles, nodule samples; diamonds, soft mat samples. Checkered samples were Sanger sequenced with *Cyanobacteria*-specific primers. General bacteria primers were used for

nodules. The calculated *chao1* diversity estimates of pyrosequenced data from corresponding depths are graphed. Photographs show different microbialite morphotypes at various depths. Black and white bars in photos from 85 feet and 106 feet are 10 cm. Photo credit: Donnie Reid.

Fig. S2 Phylogenetic tree of abundant OTUs from pyrosequencing of microbialites and Sanger sequencing of nodules with general bacteria primers. Shown are *Cyanobacteria*-related OTUs from microbialites (green), OTUs from nodule analysis (purple), Non-*Cyanobacteria* OTUs from microbialites (red). The tree was constructed using neighbor-joining method with 1000 bootstrap replicates. Bootstrap values over 60% are shown.

Fig. S3 The top 50 most abundant OTUs from microbialites and soft mats via 454 pyrosequencing and their abundance within the dataset. OTUs shaded in green are *Cyanobacteria*-related. OTUs marked with a red star are from subsection-III within the *Cyanobacteria* phylum in the SILVA database. Only six of 50 OTUs are shared (OTU-7552, OTU-11499, OTU-11510, OTU-2606, OTU-5406, OTU-12002).